RSC Advances

ROYAL SOCIETY OF CHEMISTRY

www.rsc.org/advances

Tandem dye sensitized solar cells with TCO-less back contact bottom electrode

Ajay K. Baranwal*; Tsubasa Shiki; Yuhei Ogomi; Shyam S. Pandey; Tingli Ma; Shuzi Hayase*

Kyushu Institute of Technology, 2-4 Hibikino, Wakamatsu-ku, Kitakyushu 808-0196, Japan.

A tandem dye sensitized solar cell utilizing TCO-less back contact bottom electrodes (TCO-less T-DSSC) in a novel device architecture have been reported. Owing to TCO-less bottom electrode, enhanced light absorption and photon harvesting was realized in the TCO-less T-DSSCs. In spite of the partial removal of costly TCO components, there was no detrimental effect on photon harvesting justifying the potentiality of such device architecture. Optimized TCO-less T-DSSC in this novel device architecture gave an external power conversion efficiency of 7.10 % at AM 1.5 under simulated solar irradiation.

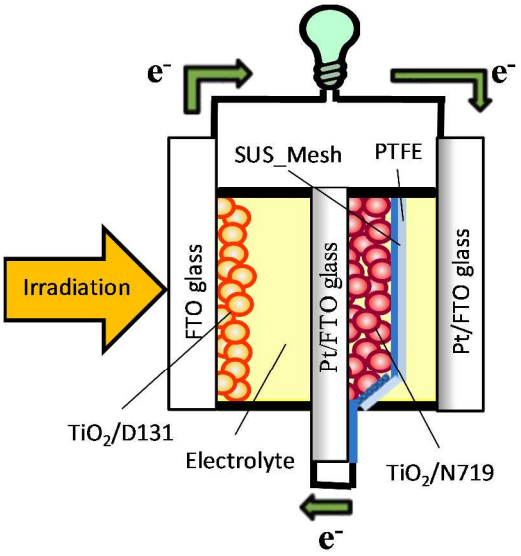

RSC Advances

RSCPublishing

ARTICLE

Tandem dye sensitized solar cells with TCO-less back contact bottom electrode

Cite this: DOI: 10.1039/x0xx00000x

Received 00th July 2014,
Accepted 00th July 2014

DOI: 10.1039/x0xx00000x

www.rsc.org/

A.K. Baranwal*, T. Shiki, Y. Ogomi, S. S. Pandey, T. Ma and S. Hayase*

We report tandem dye sensitized solar cells architecture with back contact bottom electrode (TCO-less tandem DSSC). The bottom electrode consists of glass/stained porous TiO_2/back contact porous metal. Since the structure has less transparent conductive layers (TCO layers) than simple mechanical stack tandems (Stack DSSC), the structure is capable to suppress losses of light absorption reaching the bottom electrode. Model two dyes (D131, N719) are employed to prove the tandem performances. It was proved that open circuit voltage (Voc) was the sum of Voc of the top cell and the TCO-less bottom cell, demonstrating that the cell worked as tandem cells. The power conversion efficiency of the TCO-less tandem DSSC (7.10 %) is greater than that of Stack DSSC (6.28 %).

1. Introduction

Dye Sensitized Solar Cells (DSSCs) are one of most promising third generation photovoltaic devices owing to ecological and low cost fabrication process [1-4]. Recently Grätzel and his co-workers have achieved 13% efficiency [5]. Further improvement in DSSC efficiency is needed. Enhanced light harvesting from visible to near infrared (NIR) region has been reported by panchromatic usage of sensitizer. Cocktailing different sensitizers having different photo absorption regions seems to be a promising approach, but photoconversion efficiency does not seems to be much improved [6-9]. Another prominent way to enhance photo absorption region is to employ tandem structure, where two cells are connected in series [10-13]. In tandem DSSCs (T-DSSCs), a top cell utilizes shorter wavelength region and a bottom cell harvests longer wavelength region. By matching the photocurrent density of the top and the bottom cells, the sum of open circuit voltage (Voc_{top} + Voc_{bottom}) of the top (Voc_{top}) and that of bottom cells (Voc_{bottom}) are ideally obtained. Some T-DSSCs have been reported [14-16] so far, however, almost all T-DSSCs have mechanically stacked structures. In these cells, light reaching the bottom electrode has to be pass through at least three transparent conductive oxide layers, during which photon harvesting losses occur.

T-DSSCs with TCO-glass/porous titania/dye 1/electrolyte/ dye 2/electrolyte/porous NiO/TCO-glass have been reported, where photons reaching to the bottom electrode can pass through only one TCO-glass substrate [17-18]. This provides simple T-DSSC structure, however, additional Voc is limited to about 0.1 V which is expected by the energy level difference between I_3^-/I^- redox potential and NiO valence band. Transparent Conductive Oxide less DSSCs with back contact electrode structure (TCO-less DSC) has been reported [19-20]. The TCO-less DSC is composed of glass substrate/TiO_2-dye layer/porous metal layer/electrolyte/counter electrode. The expected advantage of the TCO-less DSC is efficient light harvesting properties because light can be harvested directly without passing TCO-layers. It has been reported that the TCO-less back contact DSCs have almost the same performance as that of TCO based DSSCs [19]. By using this TCO-less structure in the bottom electrode, the number of TCO-layers can be reduced and light harvesting properties by the bottom electrode can be improved. By using the TCO-less structure, fibre type TCO-less cylindrical tandem DSSCs has been reported previously [21].

We have also reported flat T-DSSCs where photons can pass through only one TCO substrate before reaching the bottom electrode by using the back contact structure. The cell consists of TCO glass/TiO_2-dye layer (top electrode)/electrolyte/transparent Pt/compact TiO_2 /porous TiO_2 layer-dye (bottom electrode)/electrolyte/counter electrode structure. We were able to observe actually a little higher Voc than that of the corresponding single cell, however, the Voc increase was limited because of electrolyte diffusion (leaking) between top and bottom electrodes through pin holes of the compact layer fabricated in the bottom electrode [22]. Here we report TCO-less tandem DSSCs i.e. T-DSSCs architecture where bottom cell electrode has TCO-less back contact structure. These novel TCO-less T-DSSCs structures are capable to suppress absorption loss of infrared illumination (IR) by utilizing semi-transparent Pt sputtered FTO glass as an intermediate layer between top and bottom cell. This is

possible because the number of TCO layers can be reduced to one from two for simply stacked tandem cells.

2. Experimental

All materials used in the present investigation are commercially available and used without further purification. In order to fabricate tandem DSSCs by mechanically stacking top and bottom cells, corresponding photoanodes were sensitized with indoline D-131 (Mitsubishi Paper Mills, Japan) and ruthenium dye cis-bis-(isothiocyanato)bis(2,2'-bypyridyl-4,4'-dicarboxy-lato)ruthenium(II)bis-tetrabutyl ammonium (N-719, Solaronix SA), respectively. Nanoporous transparent TiO_2 paste HT/SP (Solaronix, SA) and semi-transparent paste D/SP (Solaronix, SA) were utilized for the fabrication of top and bottom photoanodes, respectively. These two dyes were selected for the sensitization of top and bottom electrodes owing their complementary light absorption properties. The chemical structures of the dyes utilized along with their electronic absorption spectra are shown in the Fig. 1. TCO-less photoanode was fabricated using flexible stainless steel mesh (SUS-730, Asada mesh Co. Ltd., Japan) having wire diameter of 13 µm with the spacing between the wire of 16 µm. A hot melt polymer film Himilan (Mitsui-DuPont Polychemicals Japan) of 30 µm thickness was used as the spacer. All the electrolytes and solvents were of reagent grade and used without any further purifications. The thickness of the nanoporous TiO_2 layer coated on the F-doped SnO_2 glass (FTO-glass) was measured using DEKTAK 6M (STYLUS PROFILER).

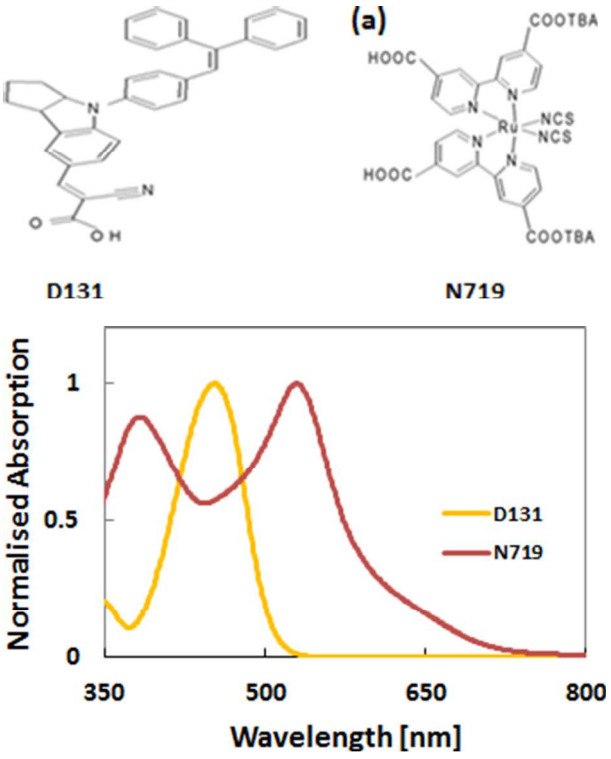

Fig 1. Chemical structure (a) and electronic absorption spectra (b) (ethanol solution) of sensitizers

2.1 Fabrication of TCO based tandem DSSC with four FTO plates (conventional mechanical tandem) as reference cells

TCO based tandem DSSC (reference cell) consisting of four TCO plates (conventional mechanical tandem) were prepared in the device configuration as follows: FTO glass/TiO_2/Dye A/electrolyte/semi-transparent Pt-FTO glass/ FTO glass /TiO_2/Dye B/electrolyte/ Pt-FTO glass which is schematically shown in the Fig. 2. Fluorine doped tin oxide (FTO) glasses were cleaned with distilled water, acetone, IPA and distilled water respectively. In addition, it was subjected to UV-ozone treatment to make the surface hydrophilic and free of organic impurities. Mesoporous TiO_2 layer of the bottom electrode was prepared by coating TiO_2 D/SP paste followed by baking at 450˚C for 30 minute. The sample was immersed in 0.3 mM solution of N-719 dye in acetonitrile: t-butyl alcohol (1:1 v/v) for 48 hrs at room temperature. Porous TiO_2 layer for the top electrode was prepared by coating TiO_2 HT/SP paste followed by baking at 450˚C for 30 minute. The sample was immersed in 0.5 mM D-131 in acetonitrile: t-butyl alcohol (1:1 v/v) for 4 hrs at room temperature for the dye adsorption. For the counter electrode of the top cell, semi-transparent catalytic Pt layer was deposited on a FTO glass by sputtering apparatus (CFS-4EP-LL, Shibaura Mechatronics, Japan). The top cell was then assembled using D131 sensitized FTO based photoanode, semi-transparent Pt-coated FTO and Himilan film spacer followed by electrolyte insertion. The bottom cell was prepared by similar process to the top cell all, except for employing N719 dye instead of D131. The tandem DSSC was then fabricated by mechanically stacking the top cell bearing D-131 sensitized photoanode and the bottom cell mentioned above. Electrolyte used for top as well as bottom cell was consisted of I_2 (50 mM), LiI (500 mM), 4-tert butyl Pyridine (580 mM) and 1-Ethyl 3-methylimidazoliumiodide (600 mM) in dehydrated acetonitrile.

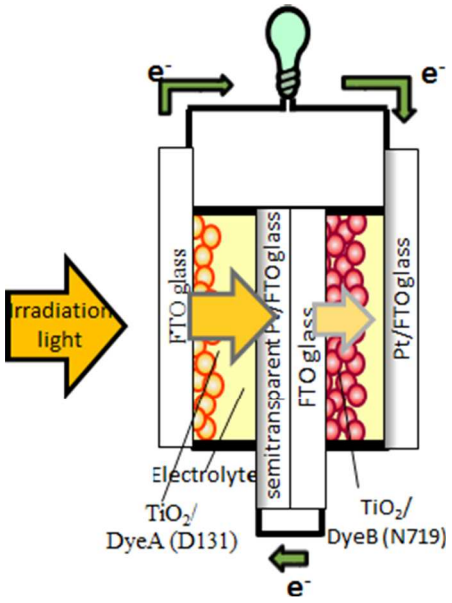

Fig 2. Schematic representation of TCO based Tandem DSSC (reference cell) having 1µm thickness top electrode and 16µm thickness bottom electrode

2.2 Fabrication of TCO-less tandem with three FTO plates

In this device architecture, one of FTO glass of bottom electrode was replaced by flexible metal mesh based TCO-less photoanode . This reduces one of the four TCO plates commonly used in standard mechanically stacked TCO based DSSCs. TCO-less tandem DSSC fabricated in this work consists of FTO glass/TiO_2-D131/electrolyte/transparent Pt-FTO glass/ N719-TiO_2/metal mesh/electrolyte/Pt-FTO glass as schematically shown in the Fig. 3. Flexible and porous metal mesh used to fabricate the TCO-less photoanode not only serves the purpose of holding the nanoporous TiO_2 layer but functions as back contact current collecting grid. Top TCO based cell sensitized with D-131 dye was prepared in the similar manner as discussed in the section 2.1. To prepare the TCO-less bottom electorde, a porous TiO_2 paste (D/SP) was screen printed on Ti (240 nm) sputtered stainless steel mesh (SUS-730) followed by baking at 450˚C for 30 min. This porous mesh coated with nanoporous TiO_2 was immersed in N719 dye bath for 48 hrs for dye adsorption. After dye absorption, samples were washed with similar solvent in order to remove residual un-adsorbed dyes. Bottom cell was prepared by assembling TiO_2 coated Ti/SUS mesh stained by N719 dye and Pt sputtered FTO glass. In order to avoid short circuit and to fill the space with electrolyte, porous polytetrafluoroethylene (PTFE) film having thickness of 35µm (H010A293D, 0.1µm pore size, ADVANTEC) was placed in between the mesh metal sheet and the Pt/FTO counter electrode. After insertion of electrolyte, both of the bottom and top cells were finally sealed with the epoxy resin. TCO-less tandem DSSC was then finally fabricated by assembling the TCO-based top electrode sensitized with D131 dye and TCO-less bottom cell sensitized with N719 dye.

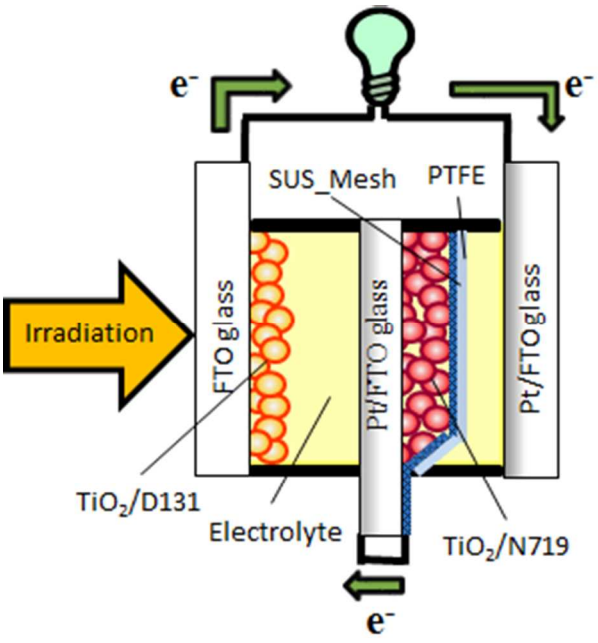

Fig 3. Schematic structure of TCO-less tandem DSSC with three FTO glass as transparent conducting substrate having 1µm thickness top cell and 16µm thickness bottom cell.

2.3 Fabrication of TCO-less tandem with two FTO plates

In order to reduce TCO component further in the tandem DSSCs, effort was made to remove both of the FTO of the bottom cell by implementing a new TCO-less device architecture. In this approach, Pt coated FTO counter electrode as mentioned in the section 2.2 was replaced by Pt coated flexible Ti metal foil. TCO-less tandem DSSCs without TCO glasses in bottom cell were fabricated in the following device architecture: FTO glass/TiO_2-D131/ electrolyte/transparent Pt-FTO glass/ N719-TiO_2-metal-mesh/electrolyte/Pt-Ti Foil as shown in Fig. 4. The basic fabrication process for individual TCO based top electrode sensitized with D131 and TCO-less N719 sensitized bottom electode was similar to that discussed earlier. Only difference in TCO-less bottom electrode lies in the removal of Pt-coated FTO counter electrode (section 2.2) by Pt sputtered Ti-foil as the counter electrode. Thickness of the sputtered catalytic Pt layer on the Pt-foil was 60 nm.

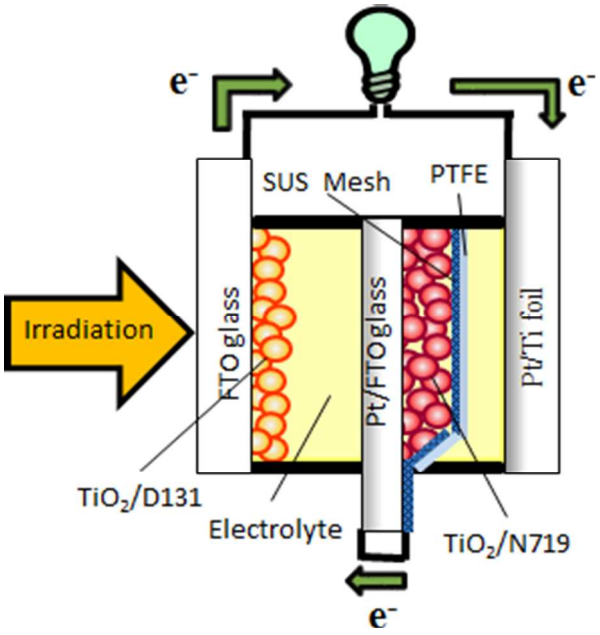

Fig 4. Schematic structure of TCO-less tandem DSSC with only two FTO glass as transparent conducting substrate. The thickness of top cell is 1µm and bottom cell has 16µm thickness.

2.4 Photovoltaic Characterizations

Photovoltaic performances were measured with solar simulator (CEP-2000 Bunko Keiki Co. Ltd, Japan) equipped with a xenon lamp (Bunko Keiki BSO-X150LC) for the light illumination. The spectrum of the solar simulator and its power were adjusted to be 100 mW/cm^2 at AM 1.5 using a spectroradiometer (LS-100, Eiko Seiki, Japan). The power of irradiated light on the solar cells was confirmed and corrected by standard amorphous silicon photodetector (Bunkokeiki BS-520 S/N 353) having similar light sensitivity to the DSSCs. Photovoltaic parameters were measured with 0.2025cm^2 mask on TiO_2 coated substrate. Photocurrent action spectra of the devices were also measured with constant photon flux of 1 X 10^{16} photons/cm^2 at each wavelength in DC mode using a photo-action spectrum measurement system connected to the solar simulator (CEP-2000, Bunkokeiki, Japan).

3. Results and discussion

3.1 Working principle of TCO-less tandem DSSC with three TCO substrates

Conventional tandem DSSCs (T-DSSCs) are stacks of two DSSCs connected in series. In the present work, T-DSSC was fabricated by using TCO-less structure as the bottom electrode, with an attempt to remove one of the TCO component from the bottom cells [19]. Figure 5 depicts electron flow in TCO-less T-DSSC consisting of TCO-based top electrode and TCO-less bottom electrode. Light is introduced from the front side. Dye (D131) in the top electrode is excited and electron is excited from $(HOMO)_{top\ electrode}$ to $(LUMO)_{top\ electrode}$, followed by injection from the dye to the porous titania layer and collected by FTO layer in the front side. The light passing through the top electrode and a FTO layer in the middle, reaches bottom electrode stained with dye N719. The bottom electrode absorbs the remaining light flux. The complementary electronic absorption spectra of dyes D131 and N719 (Fig. 1) indicates that photon longer than 500 nm which were unable to be absorbed by the top cell, are now available for the bottom cell. Electrons of N719 in the bottom electrode is excited from $(HOMO)_{bottom\ cell}$ to $(LUMO)_{bottom\ cell}$. LUMO level of dyes utilized in the present case is higher than the conduction band level of mesoporous TiO_2. This leads to the facile electron injection from dyes to porous titania. Bottom cell electrons are collected by protected metal mesh. Electrons from the top photoanode is directed to counter electrode of the bottom cell. At the same time, electrons collected by the TCO-less photoanode of the bottom cell also reaches counter electrode of the top cell. These electrons at counter electrodes reduce I_3^- in electrolytes to form I^- which lead the dye regeneration.

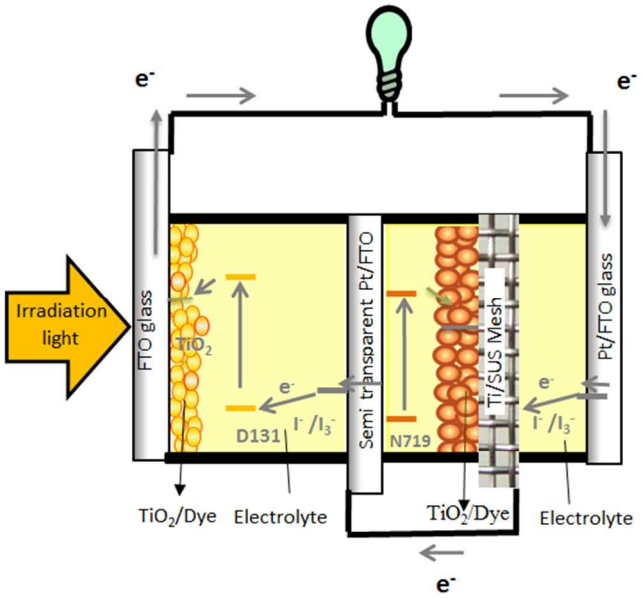

Fig 5. Schematics working principle of TCO-less tandem DSSC.

$$D + h\nu \rightarrow D^* \qquad \text{Excitation process}$$

$$D^* + TiO_2 \rightarrow e^-_{TiO_2} + D^+ \qquad \text{Injection process}$$

$$e^-_{TiO_2} + C.E. \rightarrow TiO_2 + e^-(C.E.) \qquad \text{Energy Generation}$$

$$D^+ + \frac{3}{2} I^- \rightarrow D + \frac{1}{2} I_3^- \qquad \text{Regeneration of dye}$$

$$\frac{1}{2} I_3^- + e^-_{C.E.} \rightarrow \frac{3}{2} I^- + C.E. \qquad \text{Electron recapture reaction}$$

3.2 Optimization of top cell Jsc in T-DSSCs

In series connected T-DSSCs, top cell performance in terms of its optimum thickness, light transmission through the top cell along with the complementary light absorption and photon harvesting with respect to the bottom cell play a crucial role. Since in the series connected T-DSSCs, overall efficiency is mainly controlled by the cell with the lower Jsc. Therefore, large mismatch of Jsc between bottom cell and top cell results in poor Jsc of the tandem cell. Fig 6 exhibits the photovoltaic characteristics of TCO-based single and T-DSSCs fabricated using D131 sensitized top electrode and N719 sensitized bottom electrode as the tandem DSSC device shown in Fig. 2. It can be seen from this figure that T-DSSC shows summation of the Voc of top and bottom cells which is a typical characteristics of the series connected T-DSSCs. From Table 1 it can be seen that, T-DSSC shows only a little increase in the external power conversion efficiency (4.3 %) as compared to best single cell (3.8 %, top cell). In spite of the summation of the Voc in T-DSSC, the very low FF owing to highly mismatched Jsc of the top and bottom cells could be responsible for the only slight enhancement in the photoconversion efficiency.

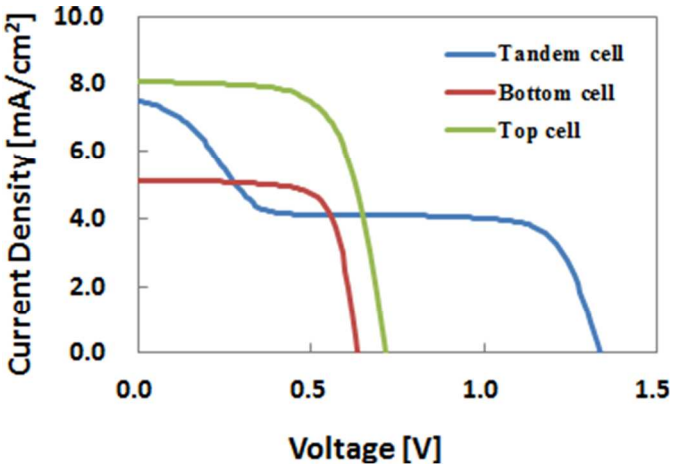

Fig 6. I-V curves for D131 sensitized top cell and N719 sensitized bottom cell along with T-DSSC (Fig 2). Thickness of the top cell nanoporous TiO_2 layer : 3 µm

Table 1. Photovoltaic parameters for single cell and T-DSSC (mechanically stacked DSSC) shown in Fig 2

	J_{sc}(mA/cm^2)	V_{oc}(V)	*FF*	η(%)
Tandem Cell	7.50	1.34	0.43	4.32
Top Cell	8.06	0.71	0.67	3.84
Bottom Cell	5.13	0.64	0.73	2.04

Since bottom cell receives only the remaining photons passing through the top cell, it is important to optimize the thickness of nanoporous TiO_2 layer used for the sensitization of D131 dye of the cells. In this context, transmission of the light through the D131 (top electrode) falling on to the bottom cell was measured with varying thickness of the nanoporous TiO_2 layer and is shown in Fig. 7. It can be clearly seen that, with increasing thickness of the TiO_2 layer in top electrode, there is decrease in the transmittance of light.

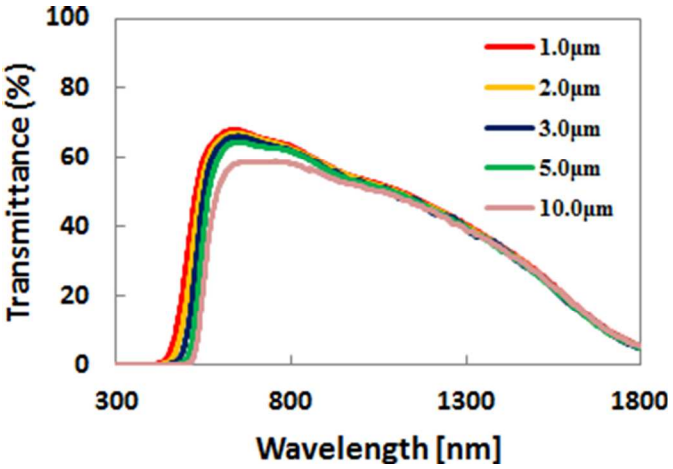

Fig 7. Change in the light transmission as a function of thickness of nanoporous TiO_2 layer of the top electrode.

Effect of the thickness of nanoporous TiO_2 layer on the photovoltaic performance of TCO-based T-DSSCs using four FTO glasses (Fig. 2) was investigated and these results are shown in Fig. 8. With the increase in thickness of top cell, the harvesting of photon flux in top cell increases. But at the same time it reduces the intensity of the transmitted light reaching the bottom cell and causes the adverse effects on the performance of bottom cell. In all cases Voc in T-DSSCs was always the sum of the Voc of respective top and bottom cell. FF was found to decrease drastically when the thickness of TiO_2 layer in the top electrode increased over 1 µm ultimately, leading to hampered overall photoconversion efficiency of the T-DSSCs with the structure of Fig. 2.

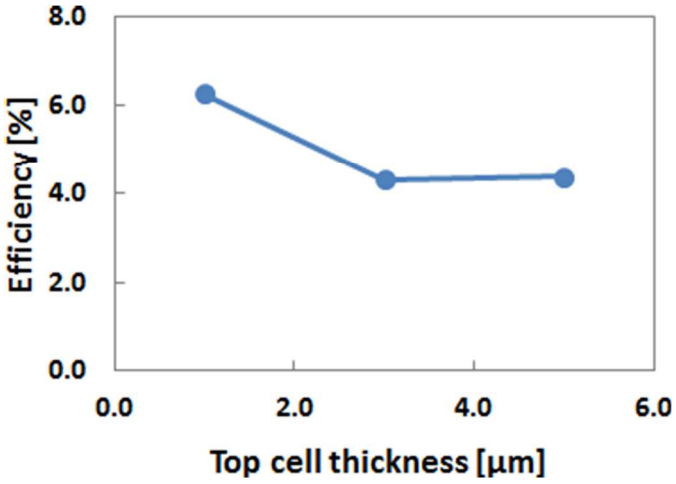

Fig 8. Relationship between thickness of nanoporous TiO_2 sensitized with D131 in top cell and photoconversion efficiency of TCO-based T-DSSCs with structure of Fig. 2.

Best photovoltaic performance (6.28%) and photon harvesting behaviour of the T-DSSC (Fig. 2) was, therefore, obtained with top cell sensitized D131 having 1µm thick nanoporous TiO_2 as shown in Fig. 9 along with the photovoltaic parameters shown in the Table 2. Table 2 clearly indicates that relatively better match between the Jsc of the top cell (7.17 mA/cm^2) and bottom cell (6.07 mA/cm^2) results in to the observation of better FF of 0.65 ultimately leading to the much improved photoconversion efficiency as compared to their individual top and bottom cells.

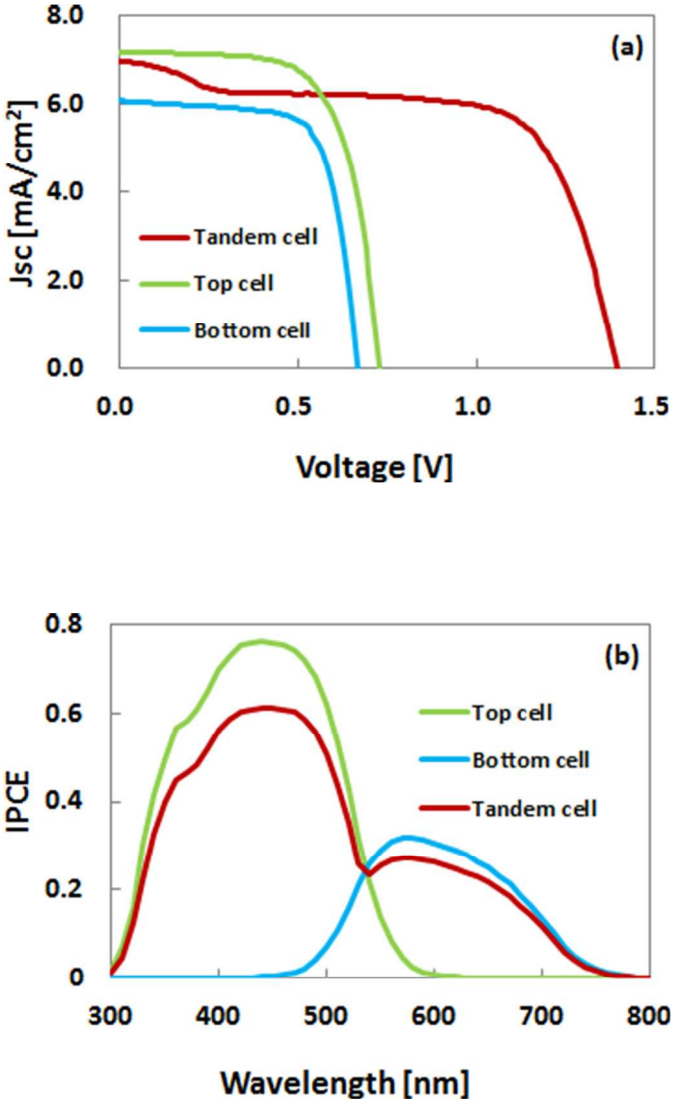

Fig 9. I-V curves (a) and photocurrent action spectra (b) for T-DSSC with structure of Fig 2 consisting of D131 sensitized top electrode and N719 sensitized bottom electrode

Table 2. Photovoltaic parameters for TCO based single top and bottom cells along with T-DSSC (Fig 2) having TiO_2 layer thickness (1 µm) in the top cell.

	J_{sc} (mA/cm^2)	V_{oc} (V)	*FF*	Efficiency (%)
Tandem Cell	6.96	1.40	0.65	6.28
Top Cell	7.17	0.73	0.67	3.53
Bottom Cell	6.07	0.67	0.71	2.89

3.3 Optimization of Jsc of bottom cell and TCO-less T-DSSC

As discussed in the section 3.2, T-DSSCs with the structure of Fig.2 usually consist of four FTO glasses. TCO is not only one of the costly components of the DSSCs but also it decreases the transmission of light when light passes from the top to the bottom [15]. TCO-less T-DSSC with the structure of Fig. 3 was fabricated and the transmission of light at the surface of bottom TiO_2 layer was compared with that of T-DSSC with the structure of Fig. 2. These results are shown in Fig. 10. It can be clearly seen that only removal of one TCO-layers of the middle substrate between top and bottom cells leads to about 20 % enhancement in transmitted light in the wavelength region of 600-1100 nm. The results suggest the usefulness of TCO-less T-DSSC device architecture in terms of available light flux to bottom cells, especially consisting of potential near infra-red sensitizers.

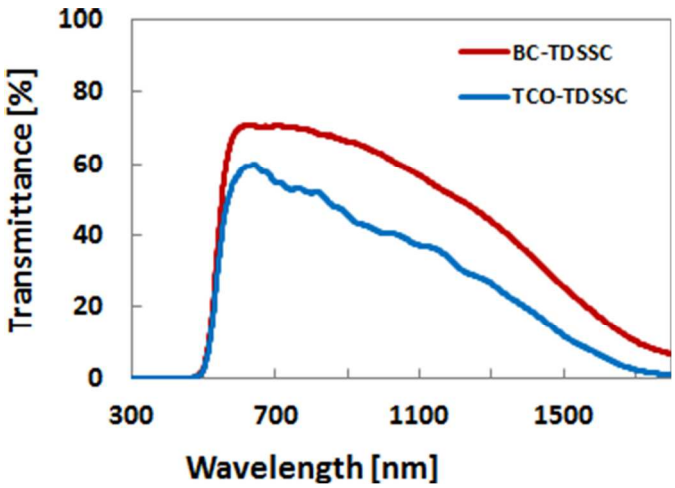

Fig 10. Transmission spectra of T-DSSC for light passing through three TCO layers (TCO-T-DSSC in Fig. 2) and only two TCO layers (BC-T-DSSC in Fig. 3)

As discussed earlier in the standard TCO based T-DSSCs with the structure in Fig. 2, nanoporous TiO_2 with 1 µm thickness gave the best performance. Optimization of the thickness for the TCO-less bottom cell sensitized with N719 dye was carried out, for TCO-less T-DSSC (Fig 3). Thickness of nanoporous TiO_2 layer coated on the protected metal mesh (bottom TCO-less electrode) was varied and the results are shown in Fig 11. In all the TCO-less T-DSSCs, about 1.45 V of Voc (just the sum of the Voc of top and bottom cells) was observed, demonstrating the tandem functionality. It is interesting to see from Fig. 11 that an optimum thickness of TiO_2 layer in TCO-less bottom electrode was 16 μ m. A relatively thinner nanoporous TiO_2 layer leads to inefficient light harvesting while much thicker TiO_2 leads redox ion diffusion limitation. As this is the same as TCO T-DSSC with the structure of Fig.2, mismatch of Jsc of the top and bottom cells leads to reduced FF of T-DSSCs, and ultimately resulting in hampered overall photoconversion efficiency.

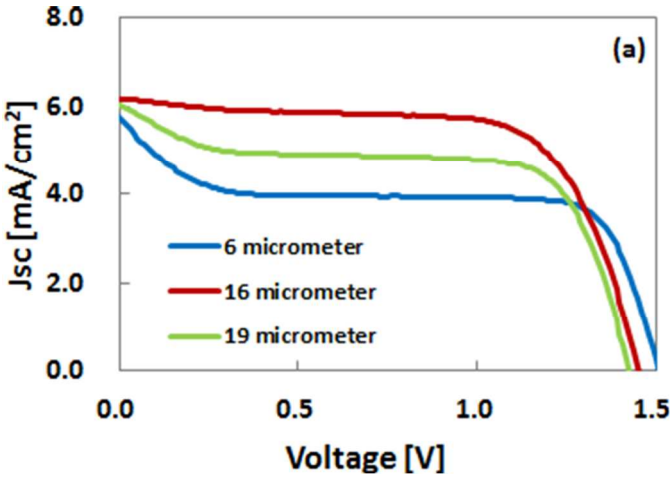

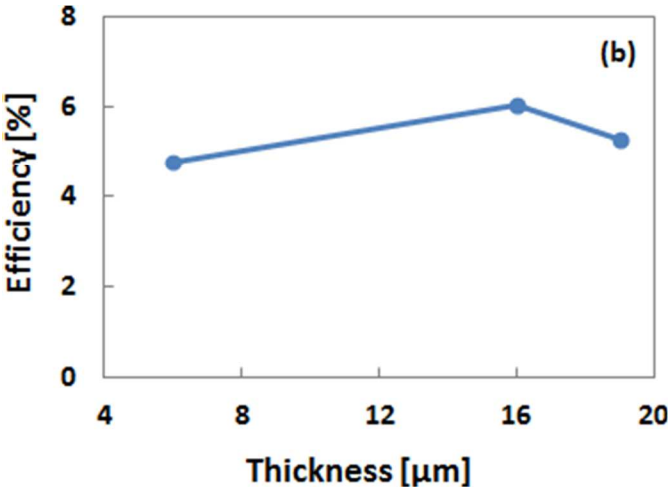

Fig 11. (a) Effect of bottom cell thickness variation on the I-V characteristics on TCO-less T-DSSCs (Fig 3) and (b) thickness dependence of bottom cell TiO_2 layer on photoconversion efficiency of TCO-less T-DSSCs (Fig. 3) .

As revealed from Fig. 11(b), best photovoltaic performance for TCO-less T-DSSC (Fig. 3) was obtained using TCO-less bottom electrode (16 µm thickness) sensitized with N719 and TCO based top electrode (1 µm thickness) sensitized with D131, as shown in the Fig. 12 and Table 3. External power conversion efficiency of 6.06 % was obtained for this TCO-less T-DSSC (Fig. 3). In addition the Voc of TCO-less T-DSSC (1.45V) is the sum of Voc observed for top cell (0.76 V) and bottom cell (0.68V), justifying the successful tandem cell formation.

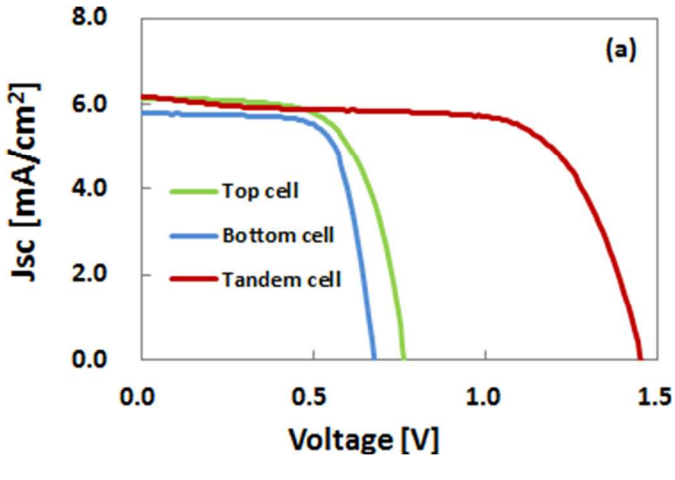

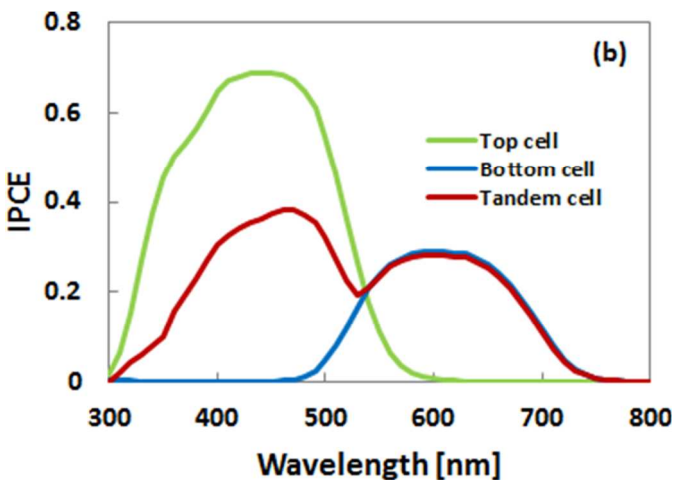

Fig 12. I-V (a) and IPCE (b) characteristics of TCO-less T-DSSC (Fig 3)

Table 3: Photovoltaic parameters of TCO-less T-DSSC (Fig 3)

	J_{sc} (mA/cm^2)	V_{oc} (V)	*FF*	Efficiency (%)
Tandem Cell	6.17	1.45	0.68	6.06
Top Cell	6.12	0.76	0.66	3.06
Bottom Cell	5.79	0.68	0.72	2.83

In the next step, in order to remove TCO layer completely from the bottom cell, TCO-less T-DSSC was fabricated using BC TCO-less bottom cell sensitized with dye N719 where Pt coated FTO was replaced with the Pt-coated Ti-foil as counter electrode in the device architecture shown in the Fig. 4. This T-DSSC contains only two TCO layers in the top cell sensitized with D131 having the optimized thickness of nanoporous TiO_2 layer (1 µm) as discussed in the previous section. Figure 13 exhibits the photovoltaic characteristics and photocurrent action spectra for TCO-less T-

DSSC with the structure in Fig. 4 along with the photovoltaic parameters shown in Table 4. A very good match of the Jsc for top and bottom cell results in to high FF of 0.69 for the TCO-less T-DSSC (Fig. 4) resulting in to the external power conversion efficiency of 7.10 %. The observation of the high Jsc and FF for the TCO-less bottom cell (Fig. 4) may be attributed to more effective use of incoming photon flux to the bottom cell utilizing the reflected light from the metallic Ti-foil. This was confirmed by the relatively higher IPCE (Fig. 13) of the TCO-less T-DSSC with the structure of Fig. 4. At the same, relatively higher conductivity of the Ti-foil as compared to the FTO results in the observation of higher FF.

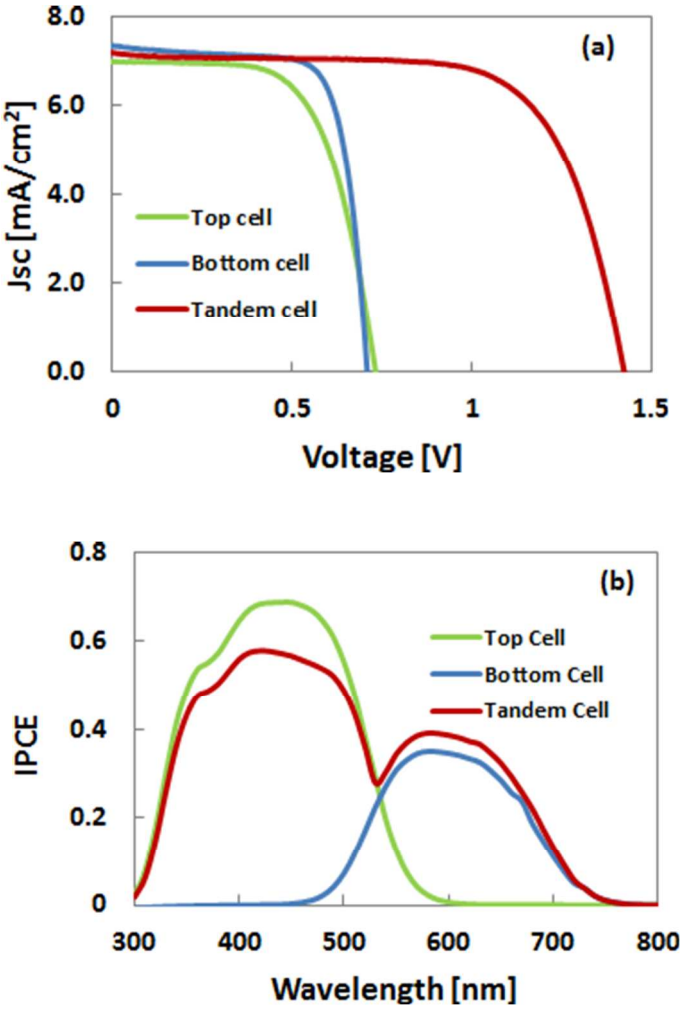

Fig 13. Photovoltaic characteristics (a) and photocurrent action spectra (b) for single cells and TCO-less T-DSSC with the structure in Fig 4

Table 4: Photovoltaic parameters of top cell, TCO-less bottom cell and T-DSSC with the structure in Fig 4

	J_{sc} (mA/cm^2)	V_{oc} (V)	*FF*	Efficiency (%)
Tandem Cell	7.20	1.42	0.69	7.10
Top Cell	7.00	0.73	0.64	3.26
Bottom Cell	7.36	0.71	0.74	3.86

4. Conclusion

TCO-less T-DSSCs were fabricated not only to remove the costly TCO components but also to enhance efficiency. The optimum thickness for the TCO-based top electrode sensitized with D131 and TCO-less bottom cell sensitized with N719 dye was found to be 1 µm and 16 µm, respectively. It was found that complete removal of the TCO layer from the bottom cell exhibited the best TCO-less T-DSSC giving Jsc of 7.20 mA/cm^2, Voc of 1.42 V and FF of 0.69 leading to the external power conversion efficiency of 7.10 %. The TCO-less T-DSSC with the structure in Fig. 4 exhibited superior photovoltaic performance to conventional TCO based T-DSSC (6.28 %) with the structure in Fig. 2. These results clearly indicate the superiority of our novel TCO-less T-DSSC architecture over previous TCO based tandem cells and justify their potentiality towards fabrication of more efficient DSSC by implementing the efficient NIR dyes for bottom TCO-less electrode.

Acknowledgements:

This work was supported by FIRST (SEGAWA) Program project and NEDO project.

Notes and references

Kyushu Institute of Technology, 2-4 Hibikino, Wakamatsu-ku, Kitakyushu 808-0196, Japan.

Email: ajaybarn@gmail.com, hayase@life.kyutech.ac.jp

Tel: (+81)80-4315-7628

1 M. Gratzel, *Journal of Photochemistry and Photobiology C: Photochemistry Reviews,* 2003, **4**(2), 145-153.
2 W. H. Thomas, A. J. Rebecca, B. F. M. Alex, Van R. Hal, T. H. Joseph, *Energy & Environmental Science,* 2008, **1**(1), 66-78.
3 M. Gratzel, *Acc. Chem. Res,* 2009, **42**, 1788-1798.
4 A. Hagfeld, G. Boschloo, L. C. Sun, L. Kloo, H. Pettersson, *Chemical Reviews,* 2010, **110**, 6595-6663.
5 S. Mathew, A. Yella, P. Gao, R. H. Baker, B. F. E. Curchod, N. A. Astani, I. Tavernelli, U. Rothlisberger, M. K. Nazeeruddin and M. Gratzel, *nature chemistry,* 2014, **6**, 242-247.
6 Y. Noma, K. lizuka, Y. Ogomi, S. S. Pandey and S. Hayase, *Japanese Journal of Applied Physics,* 2009, **48**, 020213.

7 J. Chang, C. P. Lee, D. Kumar, P. W. Chen, L. Y. Lin, K. R. J. Thomas, K. C. Ho, *Journal of Power Sources,* 2013, **240**, 779-785.
8 Y. Ogomi, S. S. Pandey, S. Kimura, S. Hayase, *Thin Solid Films,* 2010, **519**, 1087-1092.
9 J. H. Yum, S. R. Jang, P. Walter, T. Geiger, F. Nuesch, S. Kim, J. Ko, M. Gratzel, M. K. Nazeeruddin, *Chemical Communications,* 2007, **44**, 4680-4682.
10 P. Liska, K. R. Tripathi, M. Gratzel, *Applied Physics Letters*, 2006, 88, 203103.
11 W. L. Wang, H. Lin, J. Zhang, X. Li, A. Yamada, M. Konagi, J. B. Li, *Solar Energy Materials & Solar Cells*, 2010, 94, 1753-1758.
12 S. Ito, I. M. Dharmadasa, G. J. Tolan, J. S. Roberts, G. Hill, H. Miura, J.- H.. Yum, P. Pechy, P. Lisca, P. Comte, M. Gratzel, *Solar Energy*, 2011, 85, 1220-1225.
13 W. S. Jeong, J. W. Lee, S. Jung, J. H. Yun, N. G. Park, *Solar Energy Materials & Solar cells,* 2011, **95**, 3419-3423.
14 T. Kinoshita, J. T. Dy, S. Uchida, T. Kubo and H. Segawa, *nature photonics,* 2013, **7**, 535-539.
15 T. Yamaguchi, Y. Uchida, S. Agatsuma, H. Arakawa, *Solar Energy Materials & Solar Cells,* 2009, **93**, 733-736.
16 M. Yanagida, N. O. Komatsuzaki, M. Kurashige, K. Sayama, H. Sugihara, *Solar Energy Materials & Solar Cells,* 2010, **94**, 297-302.
17 J. He, H. Lindstrom, A. Hagfeldt, S. E. Lindquist, *Solar Energy Materials and Solar Cells,* 2000, 62(3), 265–273.
18 A. Nakasa, H. Usami, S. Sumikura, S. Hasegawa, T. Koyama, E. Suzuki, *Chemistry Letters,* 2005, **34**(4), 500–501.
19 Y. Kashiwa, Y. Yoshida and S. Hayase, *Applied Physics Letters,* 2008, **92**, 033308.
20 M. Z. Molla, N. Mizukoshi, H. Furukawa, Y. Ogomi, S. S. Pandey, T. Ma, and S. Hayase, *Progress in Photovoltaics*: research and Applications, 2014, doi//10.1002/pip.2526.
21 J. Usagawa, S. S. Pandey, S. Hayase, M. Kono and Y. Yamaguchi , *Applied Physics Express,* 2009, **2**, 062203.
22 K. Uzaki, S. S. Pandey, S. Hayase, *Journal of Photochemistry and Photobiology A: Chemistry,* 2010, **216**, 104-109.